scientific reports

Check for updates

OPEN

Embodied design for enhanced flipper-based locomotion in complex terrains

Nnamdi C. Chikere[1], John Simon McElroy[2] & Yasemin Ozkan-Aydin[1]✉

Robots are becoming increasingly essential for traversing complex environments such as disaster areas, extraterrestrial terrains, and marine environments. Yet, their potential is often limited by mobility and adaptability constraints. In nature, various animals have evolved finely tuned designs and anatomical features that enable efficient locomotion in diverse environments. Sea turtles, for instance, possess specialized flippers that facilitate both long-distance underwater travel and adept maneuvers across a range of coastal terrains. Building on the principles of embodied intelligence and drawing inspiration from sea turtle hatchings, this paper examines the critical interplay between a robot's physical form and its environmental interactions, focusing on how morphological traits and locomotive behaviors affect terrestrial navigation. We present a bioinspired robotic system and study the impacts of flipper/body morphology and gait patterns on its terrestrial mobility across diverse terrains ranging from sand to rocks. Evaluating key performance metrics such as speed and cost of transport, our experimental results highlight adaptive designs as crucial for multi-terrain robotic mobility to achieve not only speed and efficiency but also the versatility needed to tackle the varied and complex terrains encountered in real-world applications.

Despite significant advancements in robotic locomotion, navigating diverse landscapes for tasks such as search and rescue in complex environments (e.g., sandy terrains, wet forests, and regolith-covered landscapes), as well as responding to mudslides and avalanches, remains a formidable challenge for robotic systems[1,2]. While conventional wheeled and legged robots excel on solid ground, they often struggle on granular media such as sand, grains, or pebbles[3] due to the non-uniform and deformable nature of the terrain[4]. Moreover, factors like high resistance to penetration, instability, and limited load-bearing capacity of granular terrains can impede the mobility of these robots, leading to issues such as entrapment or slippage[5,6].

In addressing the limitations of traditional wheeled and legged robots, flipper-based locomotion offers a promising alternative. This concept draws inspiration from animals such as penguins, with their agile underwater propulsion using flippers[7,8], and seals, known for their maneuverability in both water and land[9]. Similarly, the fin-based locomotion of mudskippers, effective in terrestrial and aquatic settings, mirrors the adaptability of flipper-based systems, offering parallel insights for robotic design[10,11]. Drawing inspiration from aquatic and amphibious animals, we can equip robots with flexible and powerful flippers, enhancing adaptable propulsion and maneuverability in diverse environments, from aquatic to granular terrains[12–16].

Among the various examples of flipper-based locomotion in nature, sea turtles are particularly notable for their adeptness in traversing multiple terrains starting from a very early stage in their lives (Fig. 1—left). These animals have evolved locomotion mechanics, allowing them to navigate efficiently in water—their primary habitat—and on land, where they venture mainly for reproduction, including nesting and hatching activities[17]. Their specialized body design and unique flippers allow them to dynamically adjust to varying terrain conditions, from aquatic environments to sandy beaches and rocky shorelines[18]. This adaptability and proficiency in handling different granular media make sea turtles an ideal biological model for advancing robotic design. By studying and replicating the sea turtle's locomotion mechanics, our research aims to develop robotic systems capable of efficient navigation across various terrestrial environments (Fig. 1—right), enhancing bio-inspired robots' versatility and practical applicability.

Extensive research in bio-inspired robotics has explored various aspects of sea turtle locomotion. Biologists have focused on the distinct characteristics and biomechanical principles that facilitate their effective movement[18–20]. Concurrently, researchers in robotics have been examining techniques to replicate these characteristics in robotic designs. Recent studies have explored various aspects, from the mechanics of sea turtle-

[1]Department of Electrical Engineering, University of Notre Dame, Notre Dame, IN 46556, USA. [2]School of Mechanical and Materials Engineering, University College Dublin, Belfield, Dublin 4 D04 V1W8, Ireland. ✉email: yozkanay@nd.edu

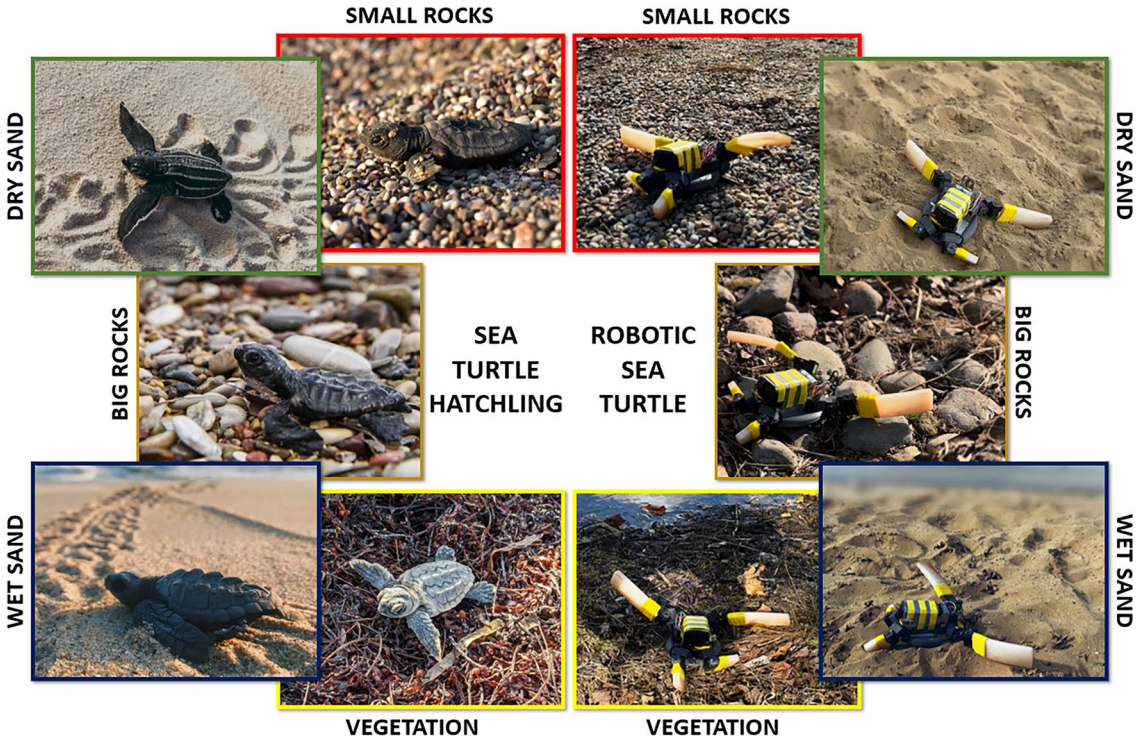

Fig. 1. Biological and robotic sea turtle hatchlings navigating diverse terrains: Sea turtle hatchling (left) and its robotic counterpart (right) are shown traversing dry sand, small and big rocks, wet sand, and vegetation, illustrating the bio-inspired robot's design effectiveness and its capability to adapt to complex environmental conditions.

inspired robots[21] to exploring the impact of different gaits of locomotion in sea turtle robots[22–24]. Mazouchova[21] found that a sea turtle-inspired robot's terrestrial movement is influenced by flipper penetration and stroke size. Zhang[25] and Zhong[26] both explored the locomotion performance of amphibious robots with transformable flipper legs, with Zhang focusing on muddy terrain and Zhong on various terrains and underwater. Both studies highlighted the importance of flipper leg rotation speed and stiffness in achieving stable locomotion. The influence of the stiffness of the flipper legs on the locomotion performance[26] as well as the load-bearing capacity associated with each locomotive gait[27] has also been investigated. More recently, Baines et al.[28] took inspiration from chelonian environmental adaptations to develop a morphing amphibious robotic limb that can switch between a streamlined flipper and a load-bearing leg, enhancing performance in both aquatic and terrestrial environments.

Findings from previous works on sea turtle-inspired robotics for real-world applications emphasize the need for ongoing research to refine their design and functionality. Despite current advancements, there remain notable gaps in the research, particularly concerning the relationship between gait patterns and flipper/body morphology across various challenging terrestrial terrains and the energy efficiency of these systems. Previous works exhibited some limitations, including the exclusive use of front flippers[21,29], reliance on a single terrestrial gait[28], notable gaps in exploring the relationship between gait patterns and flipper/body morphology for various challenging terrestrial terrains, and an analysis of the performance of the robot in only one type of terrestrial terrain. These constraints require a more holistic approach that considers the interplay between gait patterns, flipper morphology, and their implications on robotic design in various environments.

In our study, we focus on the impact of flipper/body morphology and gait patterns on the terrain adaptability of a flippered robot inspired by the morphology and locomotion mechanics of sea turtle hatchlings. A simplified robotic system (Fig. 3) was developed, tailored to function efficiently in diverse environments, specifically sand and rocky terrains. This system integrates a combination of gaits and different flipper stiffness and numbers, allowing for performance assessment in terms of average displacement and cost of transport. Our experimentation demonstrates that efficient locomotion requires distinct gait and flipper stiffness adaptations in different environments.

The findings from our study provide crucial insights into the design and control mechanisms for robotic systems aimed at emulating the locomotion of sea turtles. The unique features of our robot include its trajectory correction abilities, terrain recognition, and adaptive gait adjustments, which are coupled with the influence of morphology on its steering ability. The robot is designed to be low-cost, centimeter-scaled, robust, and autonomous, demonstrating versatile capabilities in navigation and interaction with various environments. Figure 2 offers a comprehensive overview of the conceptual framework that drives the design and application of our bio-inspired robotic sea turtle. The robot represents a significant advancement in robotics, embodying the principles of bio-inspired design and embodied intelligence to achieve deformable media locomotion as well as

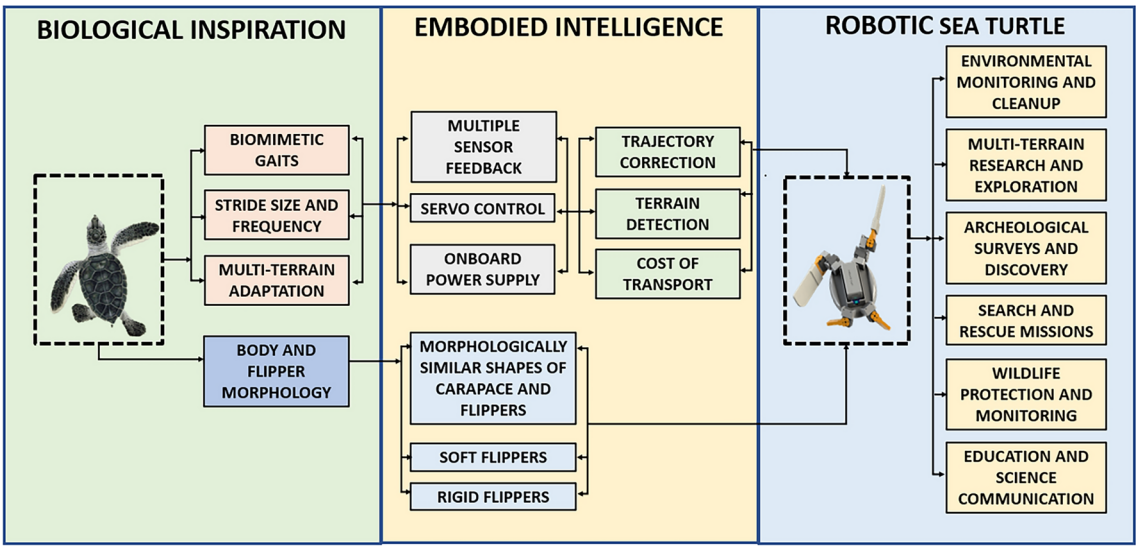

Fig. 2. Conceptual framework of the robotic sea turtle: The integrated approach combining biological inspiration with advanced robotics. The leftmost block details the biological aspects that influence the design. The center block describes the robot's embodied intelligence features, including sensor feedback, servo control, and power management. The rightmost block showcases the diverse applications of the robotic sea turtle.

terrain adaptiveness. This innovative approach enables the robot to navigate through diverse environments with the efficiency of its natural counterpart, highlighting its practical applicability in real-world scenarios such as environmental monitoring, search and rescue operations, and marine biology research. By integrating sensors, actuators, and control algorithms, the robot autonomously adapts to changing conditions, optimizing its movement through gait changes. This demonstrates the feasibility of replicating complex biological movements in robotic systems and opens new avenues for their use in scientific exploration, conservation efforts, and educational initiatives, showcasing the transformative potential of bio-inspired robotics in addressing global challenges.

Results

Biological inspiration and robot design

Drawing inspiration from the sea turtle hatchlings' morphology (Fig. 1(left)), our robot mimics their broad surface area and an upturned plastron to maintain traction and prevent sinking on soft or irregular ground. The robot's design emulates its oval body, and we incorporate interchangeable flippers (soft and rigid) for efficient terrain navigation and to investigate the impact of flipper stiffness. Additionally, the turtle's "crutching" motion is replicated to enhance stability and mobility on challenging substrates.

Studies have shown that sea turtles commonly exhibit two distinct gait patterns: the 'Cheloniid' diagonal gait and the 'Dermochelyid' all-together gait[18,30]. The 'Cheloniid' pattern, characteristic of species like the loggerhead (*Caretta caretta*), involves hatchlings using diagonally opposite limbs for crawling. This movement creates thrust through specific parts of their flippers and is a typical pattern across all Cheloniid hatchlings. On the other hand, the 'Dermochelyid' pattern observed in leatherback turtles (*Dermochelys coriacea*) consists of a "swing and stance" limb cycle, where all four flippers move together. In our work, we implement both gaits and evaluate their impact on the robot's performance.

Gait implementation

We implement two biological gait patterns on our robot, i.e., the all-together gait (Fig. 4A—top row) and the diagonal gait (Fig. 4A—bottom row). The gait sequence algorithms that imitate the motion patterns of the flippers during locomotion are shown in supplementary movie S2. The all-together gait is characterized by a simultaneous downward thrust and upward lift of all flippers. On the other hand, the diagonal gait, involving staggered actuation of diagonally opposite flippers, creates a dynamic tilt in the robot's body, ranging from a high point at the rear to a low point at the front. This results in an alternating tilt angle of roughly 20° between diagonally opposite flippers. These gaits also differ in the sequence and extent of actuation of the robotic flippers during a locomotion cycle.

The locomotion cycle and sequence are mainly governed by the actuation of the 2-degree-of-freedom (DoF) shoulder joint of the front flippers (Fig. 3A, Supplementary Figure S1A), which comprises two motors linked via a mechanism that permits the motion of the end effector, flipper, in two planes. The base motor that is connected to the body rotating within an angular range of $\alpha = -55^\circ$ (downward) to 90° (upward) in the z-plane controls the up/down rotation of the fore/aft motor (see Supplementary Figure S1B). Subsequently, the fore/aft motor governs the swing of the fore flippers in the x-plane within an angular limit of $\beta = -10^\circ$ (backward) to 75° (forward) from their neutral positions. Supplementary Figure S2 shows a plot of the trajectory of the

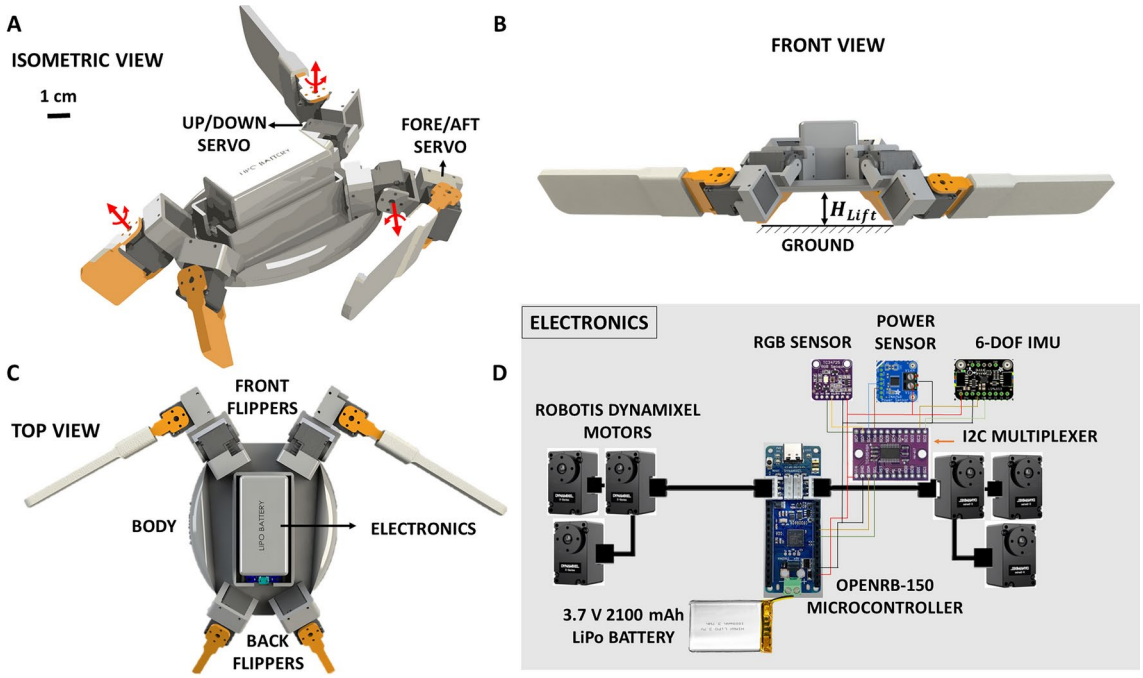

Fig. 3. Anatomical illustration of the robotic sea turtle: (**A**) Isometric CAD view, highlighting the rotation axes (red arrows) of the servos for flipper actuation. (**B**) Front view, showing the lift height of the robot above the ground. (**C**) Top view, showing the robot's symmetry and flipper arrangement. (**D**) Electronic components.

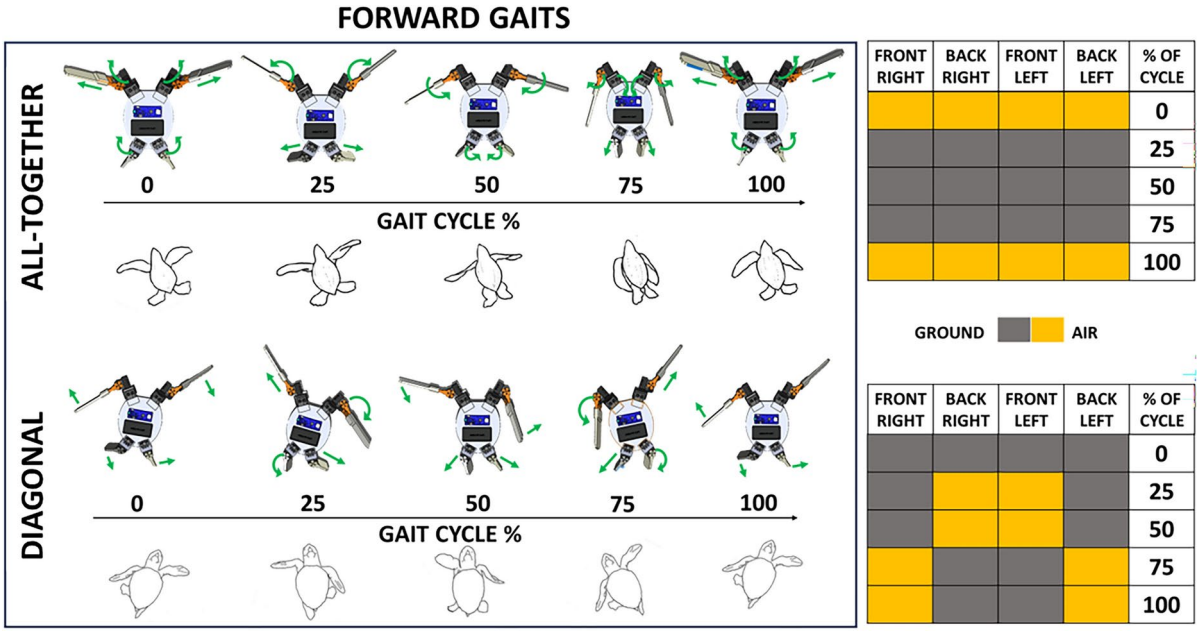

Fig. 4. Illustration of the forward gait patterns: 'All-together' (top row) and 'Diagonal' (bottom row) patterns with corresponding gait cycle diagrams. Each diagram visualizes the flipper contact with the ground (gray) and aerial phase (yellow) throughout the gait cycle. The green arrows indicate the directional movement of the flippers, emphasizing the active propulsion phases of forward and rotational movement.

servomotor's angle positions during the gaits, highlighting the synchronized movement of servos during the all-together gait and the alternating servo positions during the diagonal gait, detailed over two complete cycles. During the full upward extension of the flipper, this mechanism lifts the flipper's tip to a height of about 9.2 cm off the ground. When the flippers push down maximally during all-together gait, the robot's body (H_{Lift}

) is approximately 4 cm off the ground. The 1-DoF back flippers, responsible for directional control, rotate horizontally from $\gamma = 90^{\circ}$ to -30°.

Experimental setup and results

Experiments to investigate the locomotion mechanics were conducted on multiple terrains, including dry sand, rocky terrain (pebbles), wet sand, flat foam surface, foam stairs, and sandy inclines, as depicted in Fig. 5 and Supplementary Figure S5A. During testing, a 160x100 cm^2-bordered area for each terrain type was established to contain the robot's movement. Four main flipper configurations were examined for each gait (Supplementary Figure S5B)—the robot was equipped with either soft or rigid flippers on both ends or just on the front ends with no rear flippers.

The directional control was guided using the Inertial Measurement Unit (IMU) to ensure a consistent trajectory during locomotion, and the robot's power consumption was measured for each experimental run. Two web cameras (Logitech C920x HD Pro, 30 frames per second) were installed, one for capturing the top/back view and another for recording a side view of the robot's locomotion dynamics. The robot was positioned near one end of the border and powered on. We conducted three trials for each experiment and recorded the average displacement in terms of body length per cycle (BL/cycle) and power consumption. The best and worst performing configurations for each terrain are as shown in Fig. 5.

Dry sand tests

In dry sandy environments, our experiments (Supplementary Movie S3) compare different flipper configurations and gaits, and our results (Fig. 6A) reveal that using all flippers - whether soft or rigid - generally ensures effective locomotion. Notably, the rigid flipper setup using all-together and diagonal gaits stands out, yielding the highest measured displacement of 0.83 ± 0.03 BL/cycle. Additionally, the most energy-efficient movement, as indicated by the lowest Cost of Transport (CoT) of 9.04, was achieved with the rigid flippers in a diagonal gait. The soft flipper configuration was also effective, with displacements of 0.78 ± 0.07 BL/cycle for the all-together gait and 0.74 BL/cycle for the diagonal gait. The front-only flipper configurations recorded lower displacements ranging from 0.29 ± 0.04 to 0.51 ± 0.05 BL/cycle except the rigid front flippers with the all-together gait, which achieved a competitive displacement of 0.81 ± 0.03 BL/cycle. These results indicate that while the use of all four flippers consistently enhances locomotion effectiveness on dry sand, there is potential for optimizing the front flipper in an all-together gait in certain scenarios or specific robot designs to achieve good performance on sandy terrain.

Rocky terrain tests

Rocky terrains, with their inherent irregularities as depicted in Fig. 5 (Supplementary Figure S5A, Supplementary Movie S4), pose a significant challenge, demanding superior grip and stability for successful navigation. The terrain consisted of pebbles and rocks with sizes ranging from 3.5 to 6 cm. The rigid front flippers in an all-

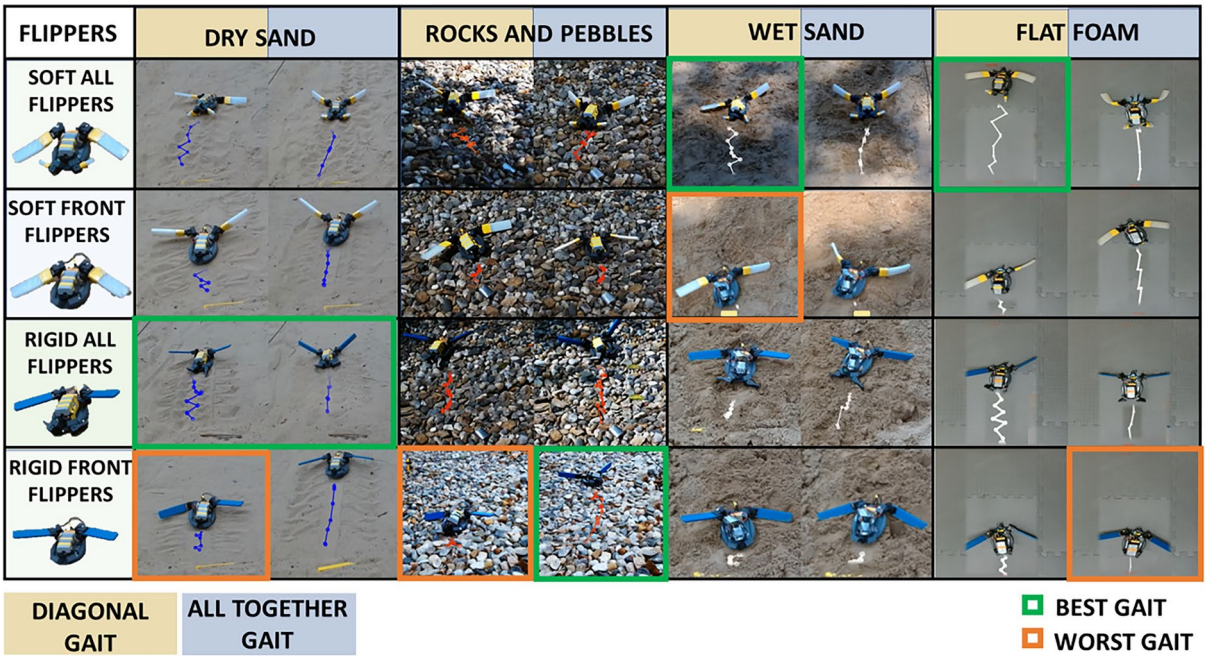

Fig. 5. Gait efficiency across varied terrains: The robot's performance with different flipper types (soft all flippers, soft front flippers, rigid all flippers, and rigid front flippers) and gait patterns (diagonal and all-together) across four terrain types: dry sand, rocks and pebbles, wet sand, and flat foam. The best and worst gaits for each flipper and terrain combination are highlighted with green and orange borders, respectively. The trajectory tracking of the robot's Center of Mass (CoM) during locomotion is shown in the blue, orange, and white lines.

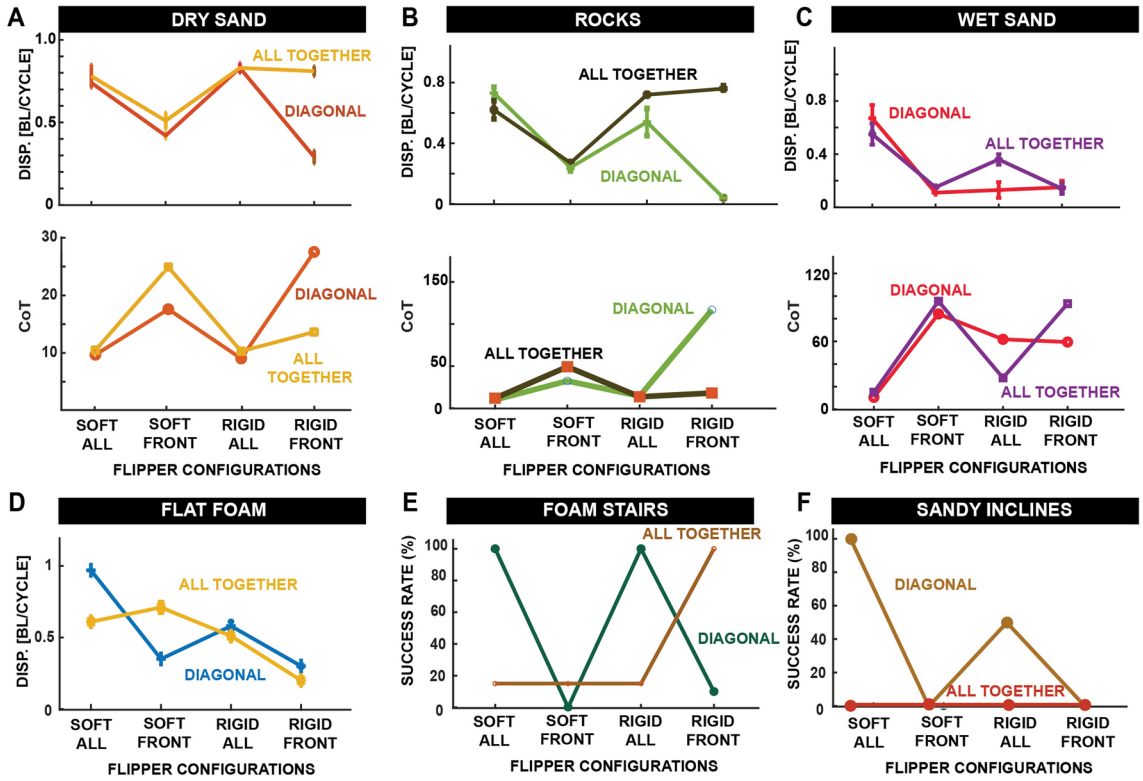

Fig. 6. Performance metrics on various terrains: The robot's CoM displacement per cycle and Cost of Transport (CoT) across different terrains with each flipper configuration (soft all, soft front, rigid, all, and rigid front) and gait patterns (diagonal and all together). (**A**) Dry sand, (**B**) Rocks, (**C**) Wet sand. (**D**) Flat foam and (**E**) Foam stairs, (**F**) Sandy inclines display success rates, illustrating the effectiveness of gait patterns in overcoming terrain obstacles.

together gait outperformed the rest with a displacement of 0.76 ± 0.02 BL/cycle (Fig. 6B). This likely stems from the gait pattern, which permits the robot to glide over the rocks, leveraging the strong support provided by the rigid front flippers. However, from an efficiency perspective, the soft flippers in a diagonal gait achieved the lowest CoT of 9.84 while also closely competing in displacement, recording an average displacement of 0.73 ± 0.04 BL/cycle. This efficiency might be due to the soft material's adaptability to the terrain's unevenness, ensuring consistent ground contact, while the diagonal gait offers balance. However, aside from the rigid front-only all-together gait, which exhibited a remarkable performance, other front-only flipper configurations underperformed in rocky terrain tests. This exception suggests that design optimizations that focus on the functionality of the front flippers could lead to enhanced locomotion in rocky environments.

Wet sand tests

The wet sand terrain (Supplementary Figure S5A, Supplementary Movie S5), reflective of real-world challenges found in cohesive granular materials such as beach sand, posed a significant challenge in our tests. Surface tension makes wet sand cohesive[31], and our results (Fig. 6C) emphasized the superiority of flipper flexibility in such conditions. Soft flippers in a diagonal gait achieved the highest displacement at 0.67 ± 0.10 body lengths (BL) per cycle and the most efficient Cost of Transport (CoT) of 10.61. This efficacy is attributed to the soft flippers' ability to contour to bumpy terrain, enhancing traction, while the diagonal gait provides consistent propulsion. The all-together gait with soft flippers also showed favorable outcomes with a displacement of 0.55 ± 0.08 BL/cycle. Conversely, rigid flippers fell behind in performance, recording a displacement of 0.13 ± 0.06 BL/cycle with the diagonal gait and 0.36 ± 0.04 BL/cycle with the all-together gait, highlighting that flipper stiffness is a detriment in moist, non-uniform terrains. Furthermore, experiments demonstrated that setups with only front flippers were less effective on wet sand for both gait patterns tested. Specifically, the configuration with soft front flippers resulted in displacements of 0.11 ± 0.00 BL/cycle and 0.15 ± 0.00 BL/cycle for the diagonal and all-together gaits, respectively. Similarly, the rigid front-only flipper setup recorded displacements of 0.15 ± 0.04 BL/cycle for the diagonal gait and 0.14 ± 0.04 BL/cycle for the all-together gait. These findings highlight the substantial impact of flipper configuration on mobility in challenging environments.

Flat foam tests

Our experiment setup on the flat foam surface consisted of a 100 x 100*cm* square foam block (Supplementary Figure S5A, Supplementary Movie S6). As shown in Fig. 6D, our results revealed varied performances for different combinations of flipper and gait. The homogeneous and predictable nature of the flat foam surface allowed for

a clear assessment of the efficiency and efficacy of each setup. The soft flippers in a diagonal gait demonstrated the highest displacement, achieving 0.97 ± 0.00 BL/cycle, with the all-together gait also performing well. Notably, configurations using only front flippers showed significant differences; the soft front flippers in an all-together gait outperformed their diagonal gait counterpart with recorded displacements of 0.71 ± 0.04 BL/cycle and 0.35 ± 0.01 BL/cycle, respectively. Rigid flippers had mixed results, with the diagonal gait yielding better displacement than the all-together gait but still falling short compared to soft flippers. The rigid front-only flippers significantly showed limited movement on this terrain, particularly in the all-together gait configuration with just 0.20 ± 0.00 BL/cycle. These results underscore the importance of flipper flexibility and movement gaits in optimizing locomotion across flat, hard surfaces.

Foam stairs tests

The experimental trials on a staircase composed of five 2.5 cm high foam blocks (Supplementary Figure S5A, Supplementary Movie S7) introduced a unique set of challenges, primarily due to the vertical ascent and climb required for successful navigation. With diagonal gait, the soft flipper configuration consistently ascended and descended the entire staircase, averaging 17 ± 3.5 cycles to complete the path and a 100% success rate. However, with the all-together gait, its ascent efficiency was reduced to a success rate of 15% due to complications arising from the interaction of the back flippers with the stairs, though descent remained unaffected with a success rate of 100%. The front-only soft flippers could not climb the stairs in either gait and with the all-together gait, it achieved a 15% ascent success rate by climbing a single stair. The rigid full flipper setup mirrored the soft flipper's performance in the diagonal gait, completing both ascent and descent with a success rate of 100%. However, the ascent success rate dropped to 15% with the all-together gait due to back flipper interference, but the descent remained successful. The front-only rigid flippers performed poorly on stairs with either gait, achieving success rate of 10% in partially ascending a single step, although their descent was successful. In summary, full flipper setups with diagonal gait performed the best (100% success rate), and front-only configurations performed poorly, as shown in the results plot in Fig. 6E.

Sandy inclines tests

The sandy inclines test setup (Supplementary Figure S5A, Supplementary Movie S8) consisted of two 20-degree angled slopes with a valley between them, simulating a real-life, challenging terrain. The soft flipper with diagonal gait successfully climbed both the hilly slopes and emerged from the valley, thus showing a 100% success rate. The success of the soft flippers with diagonal gait illustrates the configuration's capability to adapt and maintain traction on inclines. On the other hand, the soft flipper with the all-together gait failed to ascend the slopes, as the robot tended to burrow into the sand instead of ascending, indicating a need for gait modification in such conditions. Regardless of gait type, the front-only soft flipper configurations could not climb the slopes, displaying a clear shortcoming in this particular terrain with a 0% success rate. This highlights the critical need for rear flipper support in uphill tasks. Regarding the complete flipper configuration, the diagonal gait allowed the robot to ascend the first slope successfully but not climb out of the valley, resulting in a 50% success rate. Similar to the soft flipper configuration, with the all-together gait, the robot could not climb the slopes. Finally, regardless of gait type, the front-only rigid flipper configurations failed to ascend the slopes, presenting a 0% success rate. These results (Fig. 6F) show that the diagonal gait paired with a full soft flipper setup is best suited for sandy inclines, ensuring a complete success rate. In contrast, front-only setups failed across the board, underscoring the contribution of the rear flippers in overcoming steep, granular terrains.

Trajectory correction

To enhance our robot's navigational accuracy, we integrated a trajectory correction algorithm that relies on data from an Inertial Measurement Unit (IMU). This system continuously monitors the robot's orientation and acceleration to detect deviations from the set path. By processing this real-time information, the algorithm can make dynamic adjustments to the robot's movements, correcting its course to stay aligned with the planned trajectory. This feature is crucial for conducting precise experiments and maintaining effective locomotion across different terrains, where unanticipated obstacles or surface irregularities might otherwise lead to off-course travel. The trajectory correction feature functions as in Algorithm 1:

```
Initialize the Inertial Measurement Unit (IMU) and allow sensor readings to settle.
Set target_trajectory to the desired straight path.
Begin loop.
procedure TRAJECTORY CORRECTION(IMU)
    current_trajectory ← previous_trajectory + last_movement_cycle
    deviation ← CALCULATE_DEVIATION(current_trajectory, target_trajectory)
    if deviation < 15° then
        EXECUTE_MOVEMENT("Straight Gait")
    else
        scale ← CALCULATE_SCALE(deviation, max_deviation)
        if deviation is rightward then
            EXECUTE_CORRECTION("Left Correction Gait", scale)
        else
            EXECUTE_CORRECTION("Right Correction Gait", scale)
        end if
    end if
end procedure
READ_IMU_DATA
Angular_Velocity ← (Gyroscope_x, Gyroscope_y, Gyroscope_z)
Inertial_Angular_Velocity ← calculate inertial velocities from Angular_Velocity
Angle_X, Angle_Y, Angle_Z ← update angles using Inertial_Angular_Velocity and ΔT
```

Algorithm 1. Trajectory Correction

In this algorithm, the robot continually takes readings from the IMU to check whether its current trajectory is within 15° of the target trajectory. If this is the case, then the robot will continue to move forward using a 'Straight Gait.' If the current trajectory deviates from the target trajectory by more than 15°, the robot determines the direction of the deviation. Depending on whether the deviation is to the left or right, the robot will execute a correction gait - 'Right Correction Gait' for leftward deviations and 'Left Correction Gait' for rightward deviations - with the scale of correction calculated based on the magnitude of the deviation.

As the robot's body, and thus the attached IMU, does not remain level throughout its motion, simply using angle measurements calculated by the IMU to measure course deviation would not be satisfactory. These angle calculations must be performed in an "inertial reference plane," which remains level even when the robot does not. This was performed using the inertial reference frame conversion algorithm. The process repeats in a loop to maintain the correct trajectory continuously, ensuring precise navigation.

Gait transition experiments

Building on the insights from our locomotion tests, we equipped our robotic system with a feature that allows for gait transition, optimizing its movement to correspond with the detected terrain. This adaptive gait mechanism functions by a terrain recognition system that utilizes a color sensor, enabling the robot to identify different surfaces and adjust its gait accordingly.

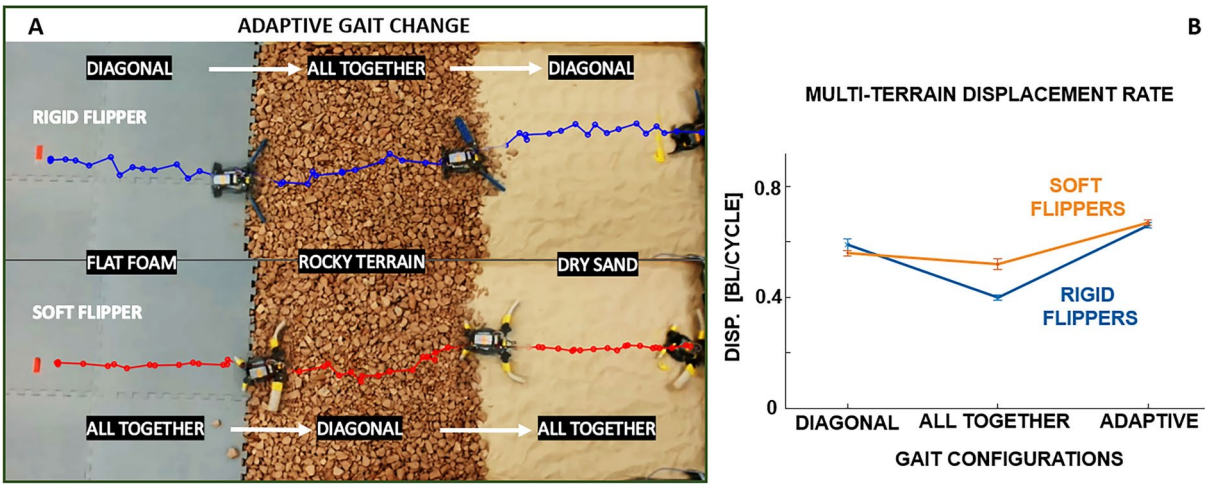

Fig. 7. (**A**) Gait adaptation: The robot's path across a segmented terrain setup, with indications of gait changes (Diagonal Gait, All Together Gait) corresponding to the type of flippers (Rigid, Soft) and the terrain encountered (Flat Foam, Rocky Terrain, Dry Sand). The Center of Mass (COM) trajectory tracking is shown in red and blue lines for the rigid and soft flippers. (**B**) Multi-terrain displacement rate: Comparison of the displacement rate in body lengths per cycle for different gait configurations (Diagonal, All Together, Adaptive) and flipper types (Soft, Rigid).

```
Initialize the color sensor on the robot.
Begin loop.
procedure ADAPTIVE GAIT(color_sensor)
    color ← DETECT_COLOR(color_sensor)
    if color is grey then
        terrain ← "Hard Ground"
    else if color is red then
        terrain ← "Rocks"
    else if color is light brown then
        terrain ← "Sand"
    else
        terrain ← "Unknown"
    end if
    gait ← SELECT_GAIT(terrain)
    EXECUTE_MOVEMENT(gait)
    return to step 4 for continuous adaptation.
end procedure
```

Algorithm 2. Sea Turtle Robot Terrain Adaptation

For practical application, we conducted a series of experiments using both rigid and soft flippers (see Fig. 7A, Supplementary Movie S9). The algorithm we developed processes input from the color sensor to identify the type of terrain. Upon terrain recognition, the algorithm selects the gait experiments shown to be most efficient for that specific surface-whether it be the diagonal gait for soft, uneven surfaces or an all-together gait for stable, flat terrains. Algorithm 2 summarises the terrain recognition and gait adaptation system.

Experiments were conducted within a confined area measuring 105 cm across, featuring segments of three different terrains: flat foam, rocks, and sand, each designated by a specific color-grey for flat foam, red for rocks, and light brown for sand. The robot's objective was to navigate this multi-terrain box, adapting its gait dynamically in response to the color sensed by its onboard sensor. Concurrently, the Inertial Measurement Unit (IMU) was utilized for trajectory correction to maintain precise navigation.

We tested the robot in both the rigid and soft flipper configurations to measure its displacement rate per cycle, focusing on the impact of the adaptive gait on performance across varying terrains compared to its performance observed when using a constant gait. As shown in Fig. 7A, the adaptive gait mechanism allowed smooth transitions between gaits, enhancing the robot's locomotive efficiency. The trajectory followed by the robot,

equipped with both rigid and soft flippers, is shown in Fig. 7A, highlighting where gait transitions occurred to accommodate different terrains.

The measured displacement rate data for both the adaptive gait changes and the single gait experiments are presented in Fig. 7B. The data reveals that for soft flippers, the 'Adaptive Gait Change' achieved the highest displacement at 0.66 ± 0.01 BL/cycle, surpassing both the 'Diagonal Gait' at 0.59 ± 0.01 and the 'All Together Gait' at 0.40 ± 0.01. The rigid flippers demonstrated a similar pattern, with the 'Adaptive Gait Change' configuration yielding the most significant displacement of 0.67 ± 0.01 BL/cycle, outperforming the 'Diagonal Gait' at 0.56 ± 0.02 and the 'All Together Gait' at 0.52 ± 0.01.

These findings verify the hypothesis that an adaptive gait mechanism, which intelligently alters locomotion strategies in real time, can optimize a robot's movement across complex and variable terrains.

Discussion

Our study examines how flipper morphology and gait patterns influence a bio-inspired flippered quadruped robot's ability to adapt to diverse terrains, taking inspiration from the locomotion of sea turtle hatchlings. The study highlights the complex interplay between mechanical design and environmental interaction necessary for proficient movement across various complex surfaces, including granular media, flat surfaces, and inclines.

Our robotic design, characterized by its low cost, robust design, and autonomous navigation capabilities, successfully emulates the versatile locomotion of sea turtle hatchlings (see Supplementary Movie S10). The biomimetic approach extends beyond mere replication of movement; it capitalizes on these creatures' inherent adaptability to navigate real-world environments effectively. By integrating sensors and adaptive algorithms, the robot demonstrates significant potential for practical applications in scenarios that mimic the challenges faced by sea turtles in their natural habitats.

Through extensive testing, we have gathered valuable data pointing to strategic combinations of flipper configurations and gaits optimized for specific environmental contexts. These findings underscore the importance of flexibility in design to accommodate the unpredictable nature of real-world terrains and set the stage for future developments in autonomous robotic systems capable of sophisticated terrain adaptation.

Our study in dry sand revealed that using all flippers, soft or rigid, regardless of gait, enables effective movement. The success of front-only rigid flippers in an all-together gait suggests that certain flipper stiffnesses could enhance locomotion on such terrain with reduced flippers. Traversing rocky terrains with their inherent irregularities and obstacles highlighted the advantages of the rigid flippers' stability and support, especially when combined with an all-together gait pattern. This configuration helped the robot maintain balance and effectively transfer force to navigate the uneven ground. Wet sand posed a different challenge; the cohesive nature of the moist substrate required a gait and morphology that prevented sinking while maintaining traction. Soft flippers in a diagonal gait emerged as superior, supporting the hypothesis that softer materials are better suited for navigating surfaces where grip and the ability to mold around uneven surfaces (malleability) are essential. The experiments on sandy inclines stressed the importance of rear flipper engagement, with full flipper configurations showing far better performance in climbing steep terrains than front-only setups. The foam stairs tests further validated this, as full flipper configurations were crucial for ascending the vertical steps, where each flipper's push-and-pull action is vital for upward propulsion.

When comparing the Cost of Transport (CoT) of our robot with other sea turtle-inspired and flipper-based robots from recent studies, notable differences emerge. On dry sand, our robot's lowest CoT of 9.04 is considerably efficient compared to the higher CoT values reported in various studies for flipper-driven terrestrial locomotion of sea turtle-inspired robots. Baines et al.[28] reported a CoT of 17.8 for the Amphibious Robotic Turtle (ART) when using a crawling gait on sand. This indicates that our robot is significantly more efficient in sandy conditions. On rocky terrain, our robot achieved a CoT of 9.84 using soft flippers in a diagonal gait. This performance is notable when compared to other studies where robots often face challenges in maintaining stability and traction on uneven surfaces. The implementation of adaptive locomotion systems, such as the artificial hormone system described by Haomachai et al.[32], has shown promise in reducing the CoT across varied terrains by responding to external environmental changes and altering robot behaviors to maintain energy efficiency. However, even with advanced systems like the one proposed by Haomachai, our robot demonstrates a significant advantage in terms of CoT, especially in rocky terrains. For wet sand, our robot's CoT of 10.61 with soft flippers in a diagonal gait also demonstrates its superior traction and stability.

Across all these terrains, the robot's ability to maintain its trajectory and autonomously adapt its gait based on terrain recognition proved essential and it's CoT performance across various terrains demonstrates its efficiency and adaptability. Implementing an adaptive gait change mechanism allowed the robot to switch between the most effective gaits for the given surface, which was particularly evident in the multi-terrain displacement rate experiments. The robotic system demonstrated proficiency in designed terrains; however, our current approach has some limitations. While controlled environments allowed for precise measurements and repeatable conditions, they did not entirely replicate real-world terrains' unpredictable and varied nature. This limitation suggests that the robot's performance in a more complex natural setting might differ, necessitating further testing in diverse, uncontrolled environments. Future iterations of this research will incorporate a broader scope of terrain types under more variable and less controlled conditions.

Reliance on color sensors for terrain recognition poses another limitation, potentially leading to inaccuracies in less controlled lighting conditions or visually uniform but texturally diverse surfaces. Augmenting the robot's perception system with other sensory inputs, such as cameras, LIDAR, radar, or even tactile sensors, could address these challenges, enabling the robot to discern and navigate more complex environments. Moreover, our approach to flipper stiffness alteration-though effective-lacks the real-time adaptive capabilities that would allow for instantaneous morphological adjustments. A robotic system capable of actively modulating its structural

rigidity similar to the robot given in previous study[28,33] in response to sensory feedback would mark a significant advancement, aligning more closely with the versatility inherent in biological organisms.

We observe that while adaptive gait changes generally enhance locomotive efficiency, the superiority of soft flippers on most terrains suggests that material compliance is often more advantageous. This aligns with the concept of "embodied intelligence" found in soft robotics[34], where the inherent properties of materials confer an ability to navigate and interact with complex environments more intuitively. Embodied intelligence emphasizes that intelligence arises not solely from a central controller but from the interaction between a robot's body and its environment, shaped by morphological parameters such as flipper compliance and material composition. Soft flippers, for example, adapt to irregular surfaces, enhancing grip and propulsion without complex control algorithms. In certain contexts, however, we find that a nuanced balance is necessary, as the structural support provided by rigid flippers proves advantageous on hard, flat surfaces. This highlights the importance of tailoring flipper properties to specific terrain types to optimize performance.

Our findings underscore the role of morphological computation, where physical properties reduce the need for extensive control, enabling efficient locomotion in diverse environments. By strategically tuning flipper compliance and geometry, we demonstrate how a robot's physical design can drive adaptive and efficient behavior, aligning with the principles of embodied intelligence. Additionally, the promise shown by the adaptive gait mechanism leads us to consider machine learning algorithms for predictive and reactive gait modulation, potentially allowing the robot to learn from its environment and further refine its locomotive strategies. By integrating a broader array of sensory data and historical performance metrics, the robot could dynamically adjust not only its gait but also predict the most suitable morphological configuration for upcoming terrain changes.

Future work would also explore incorporating aquatic locomotion capabilities, reflecting the natural proficiency of sea turtles in both land and water. The transition between terrestrial and aquatic environments remains a relatively understudied aspect in robotics, one that could greatly expand the operational range of bio-inspired designs[35–39]. Additionally, considering that our prototype emulates a sea turtle hatchling, investigating the movement of adult sea turtles and other aquatic animals with flippers could provide further valuable insights, expanding the scope and applicability of bio-inspired robotic systems in complex environments.

Overall, while this study's results are promising, they underline the need for ongoing development to overcome the current limitations and ensure that the robotic system can reliably operate in more complex and less predictable environments. The work of researchers like Ijspeert[12] and Melo et al.[13] provide further insights into the potential of exploring efficient and agile locomotion through biorobotics. Our future work will continue to build on this current study, improving our robot's design and functionality towards practical applicability. We would also explore considerations around the scalability of the design, which will be crucial for ensuring the robot's functionality across different sizes and applications.

In conclusion, the insights gained from this study contribute significantly to the field of bio-inspired robotics. Our results support the notion that while a single gait or morphology might perform well in specific conditions, adapting to the changing demands of different terrains is crucial for creating versatile robotic systems. By embodying the locomotive strategies of sea turtles, we have taken a substantial step forward in developing robotic systems capable of navigating challenging terrains. The potential applications of such technology are vast, ranging from environmental monitoring to search and rescue missions. Continued advancements in this field hold great potential to unlock new possibilities for robotic interaction with the world's most demanding environments.

Methods

Mechanical design and fabrication

The robot body (Fig. 3, Supplementary Movie S1) is designed to capture the morphological attributes of a baby sea turtle. The oval-shaped body frame, measuring 12.5 cm in length, was designed using Solidworks software and later 3D printed with a Stratasys F170 printer using Acrylonitrile Butadiene Styrene (ABS) material. The body houses the electronic components.

The robot weighs 513 grams and is equipped with four independently servo-actuated flippers; the flexible flippers were constructed using Dragon Skin™20 silicone rubber of 20A shore hardness. The rubber was mixed in a 1A:1B volume ratio and formed in a mold (Supplementary Figure S3). Larger fore-flippers (length = 12.5 cm) serve as the primary propulsion mechanism and facilitate the scooping and pushing motions essential for effective movement on various terrains. The smaller hind flippers, measuring 3.5 cm in length, aid in steering and provide additional stability and maneuverability. This anatomical differentiation between fore and hind flippers mimics the functional biomechanics of sea turtles, which use their larger front limbs for powerful strokes in water or to navigate on land and their smaller rear limbs for directional control and balance[19,40]. The use of Dragon Skin™20 silicone rubber, renowned for its durability and flexibility, ensures that the flippers can withstand the stresses of operation across different environments. The chosen shore hardness of 20A allows the soft flippers to maintain a balance between firmness and flexibility. The rigid flippers were constructed from ABS material and are the same size as the flexible flippers.

To further explore the impact of material properties, we also tested a version of the rigid flippers coated with Dragon Skin™20 silicone rubber (Supplementary Figure S6A). However, the performance of these flippers was comparable to that of the rigid flippers coated with rubber film (Plasti Dip), particularly on flat foam surfaces. Due to the ease of manufacturing and application, we opted to use Plasti Dip as the coating for the rigid flippers in our experiments.

We also tested softer flippers made from Ecoflex™30 (Supplementary Figure S6B), which has a lower shore hardness than Dragon Skin™20, offering greater flexibility. However, the Ecoflex™30 flippers bent excessively during operation, significantly limiting their ability to generate sufficient thrust. As a result, we proceeded

with configurations using rigid flippers coated with Plasti Dip and soft flippers made from Dragon Skin™20 for optimal locomotion performance across different terrains.

Electronics and control mechanism

The electronics and control mechanisms of our robot are designed to provide the required functionality for efficient and adaptive locomotion across diverse environments. The robot has six Robotis Dynamixel XL330-M288-T motors (0.42 N.m) for flipper actuation, a Robotis OpenRB-150 microcontroller for onboard control, an array of sensors to optimize its navigation and performance assessment, and a 3.7V, 2000 mAh lithium polymer battery (see Fig. 3D). The motors are well-enclosed to prevent sand damage to the gears and control the precise movements of the flippers through the angular actuation of the rotors. The sensor array includes an Inertial Measurement Unit (IMU), specifically the Adafruit LSM6DS3TR-C 6-DoF Accel + Gyro IMU, to ensure that the robot maintains a consistent travel direction, thereby improving the repeatability of experiments, a power sensor, the Adafruit INA260, measures the robot's power consumption, which is instrumental in calculating the cost of transport. In addition, a color sensor (Adafruit TCS34725) has been attached to the front part of the robot to recognize different terrains, facilitating adaptive gait transitions essential for efficient locomotion across diverse environmental conditions.

Robot kinematics

The kinematic model of our quadruped robot, inspired by the locomotive mechanisms of sea turtles, is fundamental to understanding its movement capabilities and efficiency across different terrains. This model forms the basis for analyzing the robot's movements, leading to more effective design iterations and control strategies. This model considers only the rigid flipper configuration to simplify the kinematic equations. The corresponding kinematic diagram is provided in Supplementary Figure S4.

Kinematic Configuration. Our robot's design mimics the flipper structure of a sea turtle, featuring two primary joints in each front flipper, akin to a simplified shoulder and elbow joint system. Each flipper's kinematic chain consists of two revolute joints, allowing pitch and yaw movements (Fig. 3A, Supplementary Figure S1A-B).

Joint 1—Pitch motion. The first joint, analogous to a shoulder joint, facilitates the up-and-down (pitch) motion. This joint is directly attached to the robot's body and rotates within -90 to 90 degrees. At 0 degrees, it is aligned parallel to the robot's main body.

Joint 2—Yaw motion. The second joint, like an elbow, provides the left-and-right (yaw) motion. It is connected to the first joint via a short link, which emulates the sea turtle's flipper bone structure. This joint also has a motion range of −90 to 90 degrees, and at 0 degrees, it is perpendicular to the robot's body, allowing for effective maneuvering in granular media.

Forward kinematics. The forward kinematics of each flipper are derived by considering the sequential transformations from the robot's base frame to the flipper's endpoint. Let L_1 and L_2 denote the lengths of the first and second links of the flipper, corresponding to the distance between the two joints and the length of the flipper, respectively.

Transformation matrices. Given the joint angles θ_1 and θ_2 for the pitch and yaw motions, the transformation matrices can be expressed as follows:

- Transformation from base to Joint 1 (T_1):

$$T_1 = \begin{bmatrix} \cos(\theta_1) & 0 & \sin(\theta_1) & 0 \\ 0 & 1 & 0 & 0 \\ -\sin(\theta_1) & 0 & \cos(\theta_1) & 0 \\ 0 & 0 & 0 & 1 \end{bmatrix}$$

- Transformation from Joint 1 to Joint 2 (T_2):

$$T_2 = \begin{bmatrix} \cos(\theta_2) & -\sin(\theta_2) & 0 & L_1\cos(\theta_2) \\ \sin(\theta_2) & \cos(\theta_2) & 0 & L_1\sin(\theta_2) \\ 0 & 0 & 1 & 0 \\ 0 & 0 & 0 & 1 \end{bmatrix}$$

- Transformation from Joint 2 to the flipper's endpoint (T_3):

$$T_3 = \begin{bmatrix} 1 & 0 & 0 & L_2 \\ 0 & 1 & 0 & 0 \\ 0 & 0 & 1 & 0 \\ 0 & 0 & 0 & 1 \end{bmatrix}$$

Endpoint position. The position of the flipper's endpoint relative to the robot's base frame is obtained by multiplying these transformation matrices:

$$P = T_1 \cdot T_2 \cdot T_3 \cdot \begin{bmatrix} 0 \\ 0 \\ 0 \\ 1 \end{bmatrix}$$

This results in a matrix where the first three elements of the last column represent the x, y, and z coordinates of the flipper's endpoint in the base frame.

Cost of transport

Cost of Transport (CoT) is critical in assessing locomotion efficiency, allowing meaningful comparisons across different robots and organisms[41–43]. It is a nondimensional metric defined as the ratio of power input (P_{in}) to the product of the robot's mass (m), acceleration due to gravity (g), and forward speed (v), CoT serves as a reliable measure of energy expenditure for unit mass over a unit distance (d). The formula for CoT is given as

$$COT = \frac{P_{in}}{mgv} = \frac{E_{total}}{mgd} \tag{1}$$

Where P_{in} is calculated as the sum of the power drawn from each motor on the shoulder, elbow, and hip joint, given by the formula:

$$P_{in} = \sum_{n=1}^{6} I_n V \tag{2}$$

I_n is the average current drawn from the nth motor on each joint (measured in amperes) during the gait, and V is the constant voltage supplied to the robot (3.7V). The CoT was calculated for three trials of each gait. Considering the different terrains, the gait with the lowest CoT indicated the most energy-efficient configuration.

Data availability

All data generated or analyzed during this study are included in this published article and its supplementary information files.

Received: 27 June 2024; Accepted: 21 February 2025
Published online: 05 March 2025

References

1. Rafeeq, M., Toha, S. F., Ahmad, S. & Razib, M. A. Locomotion strategies for amphibious robots—A review. *IEEE Access* **9**, 26323–26342 (2021).
2. Aguilar, J. et al. A review on locomotion robophysics: The study of movement at the intersection of robotics, soft matter and dynamical systems. *Rep. Progr. Phys.* **79**, 110001 (2016).
3. Arvidson, R. *et al.* Spirit mars rover mission: Overview and selected results from the northern Home Plate Winter Haven to the side of Scamander crater. *J. Geophys. Res.* **115** (2010).
4. Goldman, D. I. Colloquium: Biophysical principles of undulatory self-propulsion in granular media. *Rev. Modern Phys.* **86**, 943–958 (2014).
5. Qian, F. *et al. Walking and running on yielding and fluidizing ground.*
6. Reina, G. Yussof, H. (ed.) *Methods for Wheel Slip and Sinkage Estimation in Mobile Robots*. (ed.Yussof, H.) . Book Title: Robot Localization and Map Building.
7. Hui, C. A. Penguin Swimming. I. Hydrodynamics. *Physiol. Zool.* **61**, 333–343 (1988).
8. Hao, Z., Yin, B., Prapamonthon, P. & Yang, G. Hydrodynamic performance of a penguin wing: Effect of feathering and flapping. *Phys. Fluids* **35**, 061907 (2023).
9. Leahy, A. M. *et al.* The role of California sea lion (Zalophus californianus) hindflippers as aquatic control surfaces for maneuverability. *J. Exp. Biol.* **224**, jeb243020 (2021).
10. Pace, C. M. & Gibb, A. C. Mudskipper pectoral fin kinematics in aquatic and terrestrial environments. *J. Exp. Biol.* **212**, 2279–2286 (2009).
11. Swanson, B. O. & Gibb, A. C. Kinematics of aquatic and terrestrial escape responses in mudskippers. *J. Exp. Biol.* **207**, 4037–4044 (2004).
12. Ijspeert, A. J. Biorobotics: Using robots to emulate and investigate agile locomotion. *Science* **346**, 196–203 (2014).
13. Melo, K., Horvat, T. & Ijspeert, A. J. Animal robots in the African wilderness: Lessons learned and outlook for field robotics. *Sci. Robot.* **8**, eadd8662 (2023).
14. Iida, F. & Ijspeert, A. J. in *Biologically Inspired Robotics* (eds Siciliano, B. & Khatib, O.) *Springer Handbook of Robotics* 2015–2034.
15. Pfeifer, R., Lungarella, M. & Iida, F. Self-organization, embodiment, and biologically inspired robotics. *Science* **318**, 1088–1093 (2007).
16. Gravish, N. & Lauder, G. V. Robotics-inspired biology. *J. Exp. Biol.* **221**, jeb138438 (2018).
17. Hirth, H. F. Some aspects of the nesting behavior and reproductive biology of sea turtles1. *Am. Zool.* **20**, 507–523 (1980).
18. Lutz, P. L. & Musick, J. A. *The Biology of Sea Turtles, Volume I* Google-Books-ID: 5koPEAAAQBAJ.
19. Avens, L., Wang, J. H., Johnsen, S., Dukes, P. & Lohmann, K. J. Responses of hatchling sea turtles to rotational displacements. *J. Exp. Marine Biol. Ecol.* **288**, 111–124 (2003).
20. Renous, S. & Bels, V. Comparison between aquatic and terrestrial locomotions of the leatherback sea turle (Dermochelys coriacea). *J. Zool.* **230**, 357–378 (1993).
21. Mazouchova, N., Umbanhowar, P. B. & Goldman, D. I. Flipper-driven terrestrial locomotion of a sea turtle-inspired robot. *Bioinspir. Biomim.* **8**, 026007 (2013).
22. Han, B., Luo, X., Wang, X. & Chen, X. Mechanism design and gait experiment of an amphibian robotic turtle. *Adv. Robot.* **25**, 2083–2097 (2011).
23. Song, S.-H. et al. Turtle mimetic soft robot with two swimming gaits. *Bioinspir. Biomim.* **11**, 036010 (2016).
24. Wu, M. et al. A fully 3D-printed tortoise-inspired soft robot with terrains-adaptive and amphibious landing capabilities. *Adv. Mater. Technol.* **7**, 2200536 (2022).

25. Zhang, S. et al. AmphiHex-I: Locomotory performance in amphibious environments with specially designed transformable flipper legs. *IEEE/ASME Trans. Mechatron.* **21**, 1720–1731 (2016).
26. Zhong, B., Zhou, Y., Li, X., Xu, M. & Zhang, S. Locomotion performance of the amphibious robot on various terrains and underwater with flexible flipper legs. *J. Bionic Eng.* **13**, 525–536 (2016).
27. Jansen, A., Luck, K. S., Campbell, J., Amor, H. B. & Aukes, D. M. Mangan, M. *et al.* (eds) *Bio-inspired Robot Design Considering Load-Bearing and Kinematic Ontogeny of Chelonioidea Sea Turtles*. (eds Mangan, M. *et al.*) *Biomimetic and Biohybrid Systems*, 216–229.
28. Baines, R. et al. Multi-environment robotic transitions through adaptive morphogenesis. *Nature* **610**, 283–289 (2022).
29. Luck, K. S., Campbell, J., Jansen, M. A., Aukes, D. M. & Amor, H. B. From the Lab to the Desert: Fast Prototyping and Learning of Robot Locomotion (2017). ArXiv:1706.01977 [cs].
30. Wyneken, J. in *Sea Turtle Locomotion: Mechanisms, Behavior, and Energetics* Num Pages: 34.
31. Mitarai, N. & Nori, F. Wet granular materials. *Adv. Phys.* **55** (2006).
32. Haomachai, W. & Teerakittikul, P. *An Artificial Hormone System for Adaptable Locomotion in a Sea Turtle-Inspired Robot*.
33. Baines, R. L., Booth, J. W., Fish, F. E. & Kramer-Bottiglio, R. *Toward a bio-inspired variable-stiffness morphing limb for amphibious robot locomotion*, 704–710.
34. Coyle, S., Majidi, C., LeDuc, P. & Hsia, K. J. Bio-inspired soft robotics: Material selection, actuation, and design. *Extrem. Mech. Lett.* **22**, 51–59 (2018).
35. Fish, F. E. Advantages of aquatic animals as models for bio-inspired drones over present AUV technology. *Bioinspir. Biomim.* **15**, 025001 (2020).
36. Ijspeert, A. J., Crespi, A., Ryczko, D. & Cabelguen, J.-M. From swimming to walking with a salamander robot driven by a spinal cord model. *Science* **315**, 1416–1420 (2007).
37. Corucci, F., Cheney, N., Giorgio-Serchi, F., Bongard, J. & Laschi, C. Evolving soft locomotion in aquatic and terrestrial environments: effects of material properties and environmental transitions. *Soft Robot.* **5**, 475–495 (2018).
38. Wang, W., Yu, J., Ding, R. & Tan, M. *Bio-inspired design and realization of a novel multimode amphibious robot*, 140–145.
39. Baines, R., Fish, F. & Kramer-Bottiglio, R. in *Amphibious Robotic Propulsive Mechanisms: Current Technologies and Open Challenges* (eds Paley, D. A. & Wereley, N. M.) *Bioinspired Sensing, Actuation, and Control in Underwater Soft Robotic Systems* 41–69.
40. Renous, S., Bels, V. & Davenport, J. Locomotion in marine Chelonia: Adaptation to the aquatic habitat. *Historical Biol.* **14**, 1–13 (2000) .
41. Von Karman, T. What price speed? specific power required for propulsion of vehicles. *Mech. Eng.* **72**, 775 (1950).
42. Tucker, V. A. The Energetic Cost of Moving About: Walking and running are extremely inefficient forms of locomotion. Much greater efficiency is achieved by birds, fish-and bicyclists. *Am. Scientist* **63**, 413–419 (1975).
43. Gregorio, P., Ahmadi, M. & Buehler, M. Design, control, and energetics of an electrically actuated legged robot. *IEEE Trans. Syst. Man Cybern. Part B* **27**, 626–634 (1997).

Acknowledgements

We would like to thank the Naughton Undergraduate Fellowship program for supporting John McElroy. We would also like to express our appreciation to Dr. Frank Fish and the members of Notre Dame MiNiRo-Lab for their invaluable contributions and insightful discussions.

Author contributions

Y.O.A. designed the study, N.C. and J.M. built the robot. N.C. performed the experiments with the assistance of J.M., N.C. and Y.O.A. analyzed the experimental data. N.C. and Y.O.A. wrote the manuscript and critically reviewed the manuscript. All authors approved the final manuscript, taking responsibility for all aspects of the work to ensure that any concerns regarding accuracy or integrity are thoroughly addressed.

Declarations

Competing interests

The authors declare no competing interests.

Additional information

Supplementary Information The online version contains supplementary material available at https://doi.org/10.1038/s41598-025-91948-3.

Correspondence and requests for materials should be addressed to Y.O.-A.